Science Bulletin xxx (xxxx) xxx

Contents lists available at ScienceDirect

Science Bulletin

journal homepage: www.elsevier.com/locate/scib

Short Communication

Topographic, cognitive, and neurobiological profiling of the interdependent structural and functional modules of the brain

Xiaoyue Wang [a], Lianglong Sun [b,c,d,*], Xinyuan Liang [b,c,d], Tengda Zhao [b,c,d], Mingrui Xia [b,c,d], Xuhong Liao [e], Yong He [b,c,d,f,*]

[a] School of Medical Technology, Beijing Institute of Technology, Beijing 100081, China
[b] State Key Laboratory of Cognitive Neuroscience and Learning, Beijing Normal University, Beijing 100875, China
[c] Beijing Key Laboratory of Brain Imaging and Connectomics, Beijing Normal University, Beijing 100875, China
[d] IDG/McGovern Institute for Brain Research, Beijing Normal University, Beijing 100875, China
[e] School of Systems Science, Beijing Normal University, Beijing 100875, China
[f] Chinese Institute for Brain Research, Beijing 102206, China

ARTICLE INFO

Article history:
Available online xxxx

The structural and functional connectomes interact and depend on each other to jointly maintain the functioning of the brain and further support cognitive processing. Elucidating the complex interplay between the structural connectome (SC) and functional connectome (FC) is one of the central challenges in network neuroscience. While previous studies have consistently reported SC-FC coupling or SC constraints on FC [1–3], they typically analyzed these networks in isolation. Interdependent network theory [4] provides an important mathematical framework for studying network interactions, revealing nontrivial properties such as overabundant network motifs or subgraphs [5], core hub regions [6], core-periphery structures [7], and assortative mixing patterns [8] in the multilayer SC-FC connectome. However, how the SC and FC layers are topographically coordinated by different nodes in the interdependent connectome and how such multilayer coordination contributes to cognitive processes remain to be elucidated. Moreover, the neurobiological basis of the interdependent SC-FC connectome remains unknown. It is particularly important to answer these questions to better understand the organizational principles of interdependence in the unified SC-FC connectome and to elucidate the underlying biological mechanisms that govern the connectome.

Brain modularity is a fundamental topological property in both structural and functional domains, yet the correspondence between modular organizations across these network types remains poorly understood. To address this issue, we leveraged multimodal resting-state functional magnetic resonance imaging (MRI) and diffusion MRI data from 1012 healthy participants from the Human Connectome Project (HCP) S1200 dataset [9] (For details, see Supplementary Materials). Using a surface-based multimodal parcellation atlas [10] with 360 cortical areas, for each individual we constructed FC networks based on Pearson correlations between the time series of all pairs of nodes and SC network using the probabilistic diffusion tractography. We then modeled the interplay between the SC and FC in a multiplex framework that establishes interlayer connections based on direct correspondence between identical nodes. This process resulted in a two-layer interdependent SC-FC network for each individual, represented by a supra-adjacency matrix where the diagonal blocks represent the intralayer connections and the off-diagonal blocks correspond to the interlayer connections. We applied multilayer modularity detection algorithm [11] to simultaneously analyze both layers, generating consistent community labels and enabling direct comparison of SC-FC modular organization. The difference in modular architecture between SC and FC layers was quantified using multilayer modular variability [12], where higher values (e.g., node A in Fig. 1a) indicate greater differences in the module structures to which nodes belong in the SC and FC layers.

For each individual, we identified multilayer connectome modules and computed multilayer modular variability in the SC-FC connectome (Fig. 1b). Details on other network topological measures and their relationships with multilayer modular variability are provided in the Supplementary Materials. The group-level multilayer modular variability showed substantial spatial heterogeneity across the cortex, with greater variability predominantly in the lateral prefrontal and parietal regions, dorsal medial prefrontal cortex, and lateral temporal regions and less variability in the sensorimotor, visual, and ventral medial prefrontal cortex (Fig. 1c). Furthermore, we investigated whether the spatial pattern of group-level multilayer modular

* Corresponding authors.
E-mail addresses: lianglongsun@mail.bnu.edu.cn (L. Sun), yong.he@bnu.edu.cn (Y. He).

https://doi.org/10.1016/j.scib.2025.02.029
2095-9273/

Please cite this article as: X. Wang, L. Sun, X. Liang et al., Topographic, cognitive, and neurobiological profiling of the interdependent structural and functional modules of the brain, Science Bulletin, https://doi.org/10.1016/j.scib.2025.02.029

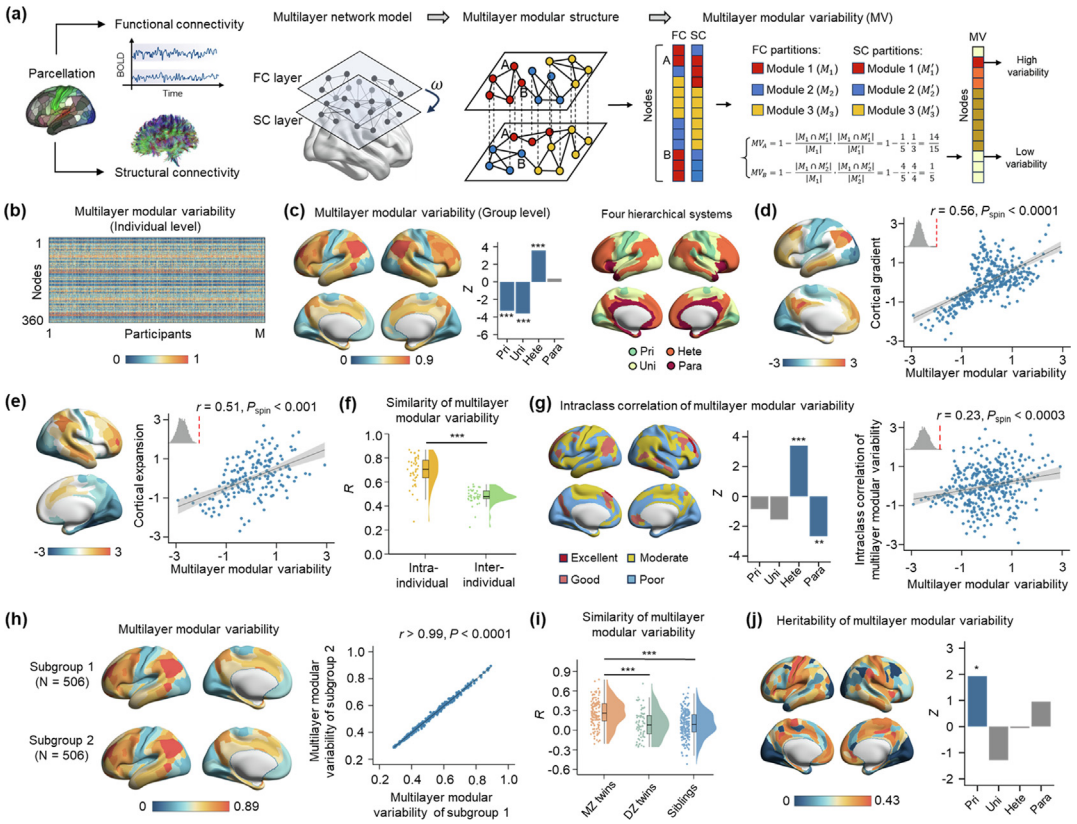

Fig. 1. Spatial topography and its test–retest reliability and heritability of multilayer modular variability in the interdependent SC-FC connectome. (a), Schematic of SC-FC connectome construction and multilayer modular variability (MV) calculation. (b), Multilayer modular variability at individual-level. (c), The spatial topography of group-level multilayer modular variability and its correlations with the functional connectivity gradient (d) and evolutionary expansion of cortical surface area (e). (f), Similarity of multilayer modular variability of intra-individual and inter-individual. (g), Spatial topography of intraclass correlation and its correlation with multilayer modular variability. (h), Correlation of multilayer modular variability between two half-split subgroups. (i), Similarity of multilayer modular variability among monozygotic, dizygotic and siblings pairs. (j), Spatial distribution of multilayer modular variability heritability. Bar plots show values in four hierarchical systems, with colored bars indicating cortical systems differing from null model. In scatter plots, gray shading represents 95 % confidence interval, upper-left histograms show null-model r values, and red dotted lines indicate empirical r values. Each dot represents the mean value of node across participants. To better visualize the scatter plots, the raw values were scaled using a rank-based inverse Gaussian transformation. Pri, primary cortex; Uni, unimodal cortex; Hete, heteromodal cortex; Para, paralimbic cortex. MZ, monozygotic; DZ, dizygotic. * $P < 0.05$, ** $P < 0.01$, *** $P < 0.001$.

variability represents cortical hierarchical organization. First, we stratified the 360 cortical regions into four hierarchies illustrating a transition from primary sensory regions to the transmodal cortex. The heteromodal system (Spin test P value (P_{spin}) < 0.001) exhibited greater variability, while the primary (P_{spin} = 0.0003) and unimodal (P_{spin} < 0.001) systems exhibited less variability (Fig. 1c). Second, we found that the topographic organization of group-level multilayer modular variability correlated with a well-established macroscale connectome gradient architecture from unimodal to transmodal (r = 0.56, P_{spin} < 0.0001, confidence interval (CI) = [0.48, 0.62], two-tailed; Fig. 1d). Given that greater variability was observed in the association regions that are thought to be phylogenetically late-evolving regions, we examined its relationship with cortical evolutionary expansion. We found a significant positive correlation (r = 0.51, P_{spin} < 0.001, CI = [0.39, 0.61], two-tailed; Fig. 1e), where highly expanded transmodal areas exhibited greater variability than conserved sensory areas. These results suggest that the modular topography of multilayer SC-FC connectome varies along the primary-to-transmodal axis and reflects cortical evolutionary expansion.

We further assessed the reliability, reproducibility, and heritability of multilayer SC-FC connectome. Using the HCP Test-Retest dataset (42 participants, aged 30.4 ± 3.33 years, 30 females), we calculated the Pearson correlation of multilayer modular variability across test–retest sessions and found significantly higher intraindividual similarity (r: 0.69 ± 0.123, nonparametric permutation test P value (P_{perm}) < 0.0001) compared to interindividual similarity (r: 0.48 ± 0.065; Fig. 1f). Furthermore, for each brain node, we performed the intraclass correlation (ICC) analysis to estimate its test–retest reliability of the multilayer modular variability. This analysis revealed highest test–retest reliability in dorsolateral prefrontal and inferior parietal cortex (ICC > 0.6), with the heteromodal system showing greater reliability than null model (P_{spin} < 0.001) and the paralimbic system showing lower reliability (P_{spin} = 0.0039; Fig. 1g). The ICC map correlated with group-level modular variability (r = 0.23, P_{spin} < 0.0003, CI = [0.13, 0.32], two-tailed; Fig. 1g). We also performed reproducibility analysis using random split-half sampling procedure (1000 repetitions) in which the HCP S1200 dataset was divided into two cohorts (Subgroup 1 and 2). The group-level multilayer modular variability showed high correlation between subgroups (r: 0.994–0.999, P < 0.0001; Fig. 1h). Finally, using twin and family data (268 monozygotic twins, 140 dizygotic twins, 107 singletons, and 494 nontwins), we showed higher similarity in multilayer modular variability among monozygotic twins (r: 0.26 ± 0.204) compared to dizygotic twins (r: 0.10 ± 0.217, P_{perm} < 0.0001) and siblings (r: 0.10 ± 0.196, P_{perm} < 0.0001; Fig. 1i). Heritability analysis (For details, see Supplementary Materials) revealed that genetic factors exerted a regionally variable influence on multilayer modular variability, with higher heritability in the somatosensory, lateral temporal,

medial prefrontal, and parietal regions and lower heritability in the lateral frontal and parietal regions and visual cortices (Fig. 1j). Similarly, primary system showed higher heritability compared to null models (P_{spin} = 0.016; Fig. 1j).

Next, we investigated the relationship between SC-FC interaction and neurocognitive flexibility. Based on Yeo et al.'s cognitive components [13], we calculated the neurocognitive flexibility of each node by averaging the number of cognitive components of all voxels within that node. We found a significant correlation between group-level multilayer modular variability and neurocognitive flexibility (r = 0.27, P_{spin} = 0.004, CI = [0.17, 0.36], two-tailed; Fig. 2a). After categorizing brain nodes into four flexibility levels (Low: 0–1, moderate: 1–2, good: 2–3, high: ≥ 3 components) based on cognitive component count, high flexibility nodes exhibited high multilayer modular variability (Kruskal-Wallis test, Bonferroni correction, P < 0.001; Fig. 2a). This suggests that nodes with higher multilayer modular variability tend to participate in multiple cognitive components, contributing to higher cognitive flexibility. We further investigated the relationship between multilayer modular variability and individual's cognitive function. Using multivariate partial least squares (PLS) analysis, we examined this relationship in the primary and transmodal cortices. Specifically, we first stratified the cerebral cortex into low-order area (Primary and unimodal regions, 176 regions in total) and high-order transmodal area (Heteromodal and paralimbic regions, 184 regions in total). PLS analysis revealed no significant relationship in the low-order cortex, while in transmodal cortex, the first latent variable (LV1) significantly (P_{perm} < 0.0008) captured 46% of the covariance between multilayer modular variability and cognition (Fig. 2b). Under the LV1, the multilayer modular variability score was correlated with the cognition score (r = 0.24, P_{perm} = 0.001, CI = [0.19, 0.30], two-tailed; Fig. 2b). This correlation was determined by the brain regions and cognitive terms contributing most to the LV. Therefore, we computed the loadings to determine the

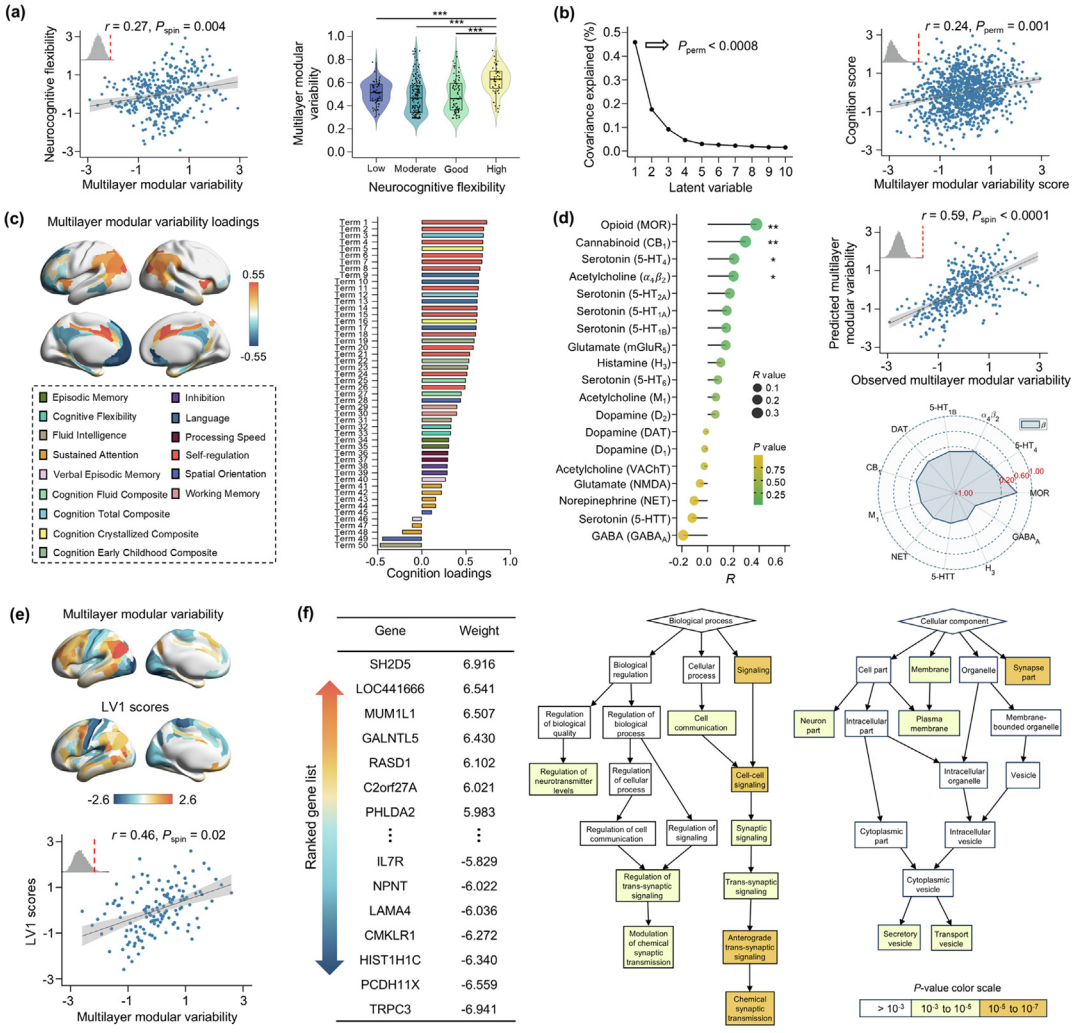

Fig. 2. Cognitive and molecular associations of multilayer modular variability in the interdependent SC-FC connectome. (a), Correlation between multilayer modular variability and neurocognitive flexibility, shown via violin plot for nodes with low to high flexibility. (b), Partial least squares (PLS) analysis between individual multilayer modular variability and cognitive measures. First PLS latent variable (LV1) shows optimal linear combination of brain regions covarying with cognitive scores (46% covariance explained). For LV1, the multilayer modular variability score and cognition score were correlated. Detailed methods are presented in Supplementary Methods 2.8. (c), Significant loadings of brain regions and cognition terms (1000 bootstrap repetitions). Cognitive processes shown in left panel's dashed box with color coding. Full cognitive details in Table S2 (online). (d), Left panel depicts the correlation between receptors/transporters and multilayer modular variability. Scatter plot shows the prediction results of the elastic net regression. Radar Chart displays significant predictive features with regression coefficients (β). (e), Multivariate PLS regression analysis between group-level multilayer modular variability and gene expression. LV1 component captures dominant covariation between regional modular variability and transcriptomic patterns, showing a significant correlation with multilayer modular variability. Detailed methods are presented in Supplementary Methods 2.10. (f), Gene ontology enrichment analysis results from gene list (details in Table S3 (online)). Each dot in scatter plots of (a), (d) and (e) represents the mean value of node across participants. In scatter plot of (b), dots represent individual participant scores on the latent components of brain and cognitive measurements.

degree of contribution of each variable and assessed its reliability (1000 bootstrap repetitions). For multilayer modular variability, regions with large positive loadings were mainly in the inferior parietal cortex, temporal-parietal-occipital junction, and anterior cingulate cortex, whereas regions with large negative loadings were mainly in the medial prefrontal, posterior cingulate, and lateral temporal cortices (Fig. 2c). Cognitive terms showed predominantly positive loadings, particularly in self-regulation, cognition total composite, and cognition crystallized composite cognitive processes (Fig. 2c and Table S2 online). These results demonstrated that greater multilayer modular variability in brain regions with positive loadings was associated with better high-level cognitive performance.

To elucidate the neurobiological underpinnings of the coupled SC-FC connectome, we analyzed associations with neurotransmitter systems [14] and gene expression [15]. (i) We first obtained cortical distribution data of 19 neurotransmitter receptors/transporters from nine neurotransmitter systems [14]. Then, we calculated the average density of each receptor/transporter of each cortical region, finding significant correlations between group-level multilayer modular variability and MOR (r = 0.38, P_{spin} < 0.0001, CI = [0.28, 0.46], two-tailed, with FDR correction), CB_1 (r = 0.29, P_{spin} < 0.0002, CI = [0.20, 0.38], two-tailed), 5-HT_4 (r = 0.20, P_{spin} = 0.0087, CI = [0.10, 0.30], two-tailed) and $\alpha_4\beta_2$ (r = 0.20, P_{spin} = 0.0042, CI = [0.10, 0.30], two-tailed) receptors (Fig. 2d and Fig. S2a online) Using the multivariate elastic net regression model (λ = 0.011; Fig. S2b online), we found that receptor and transporter distributions could predict modular variability pattern (r = 0.59, P_{spin} < 0.0001, CI = [0.52, 0.66], two-tailed; Fig. 2d and Fig. S2c online). 11 receptors/transporters contributed to the prediction model (Fig. 2d), with MOR, 5-HT_4, and $\alpha_4\beta_2$ having the highest contributions. The robustness of these findings was further validated using LASSO regression (Fig. S3 online; for details, see Supplementary Results 3.3). Together, our results highlighted the tight link between the interdependent SC-FC connectome and multiple neurotransmitter systems. (ii) Using regional microarray expression data from the Allen Human Brain Atlas (AHBA) dataset (6 donor brains) [15], we investigated whether the multilayer module configuration was associated with gene expression profiles. PLS regression analysis revealed that the LV1, explaining 21.25% of multilayer SC-FC modular variability (P_{spin} = 0.02; Fig. S4 online), significantly correlated group-level multilayer modular variability with regional gene expression (r = 0.46, P_{spin} = 0.02, CI = [0.31, 0.59], two-tailed; Fig. 2e). The LV1 component represented a gene expression profile with high expression mainly in the lateral frontal and parietal cortices but low expression in the sensorimotor and visual cortices. We then performed Gene Ontology (GO) enrichment analysis on genes associated with the transcriptome features of the LV1 component. Genes ranked by weight from most positive to most negative were enriched in biological processes related to chemical synaptic transmission and cellular components related to synapse part, plasma membrane, neuron part, transport vesicle, and secretory vesicle (FDR-corrected, all q < 0.05; Fig. 2f and Table S3 online). No significant enrichment was observed for molecular function. These patterns reflect adaptive mechanisms in higher-order cognitive regions, where complex neural connections and flexible SC-FC relationships support functional diversity. The high expression of genes involved in neural signal transmission enables dynamic SC-FC adjustments, ultimately leading to higher variability in cross-layer modular organization. We also performed GO enrichment analysis on inversely ranked genes (Table S4 online). Collectively, these results revealed a potential molecular basis for the multilayer module organization in the interacting SC-FC connectome.

Our results are highly robust to confounding factors such as head motion, connectivity thresholds, network construction methods, prediction model, and parcellation schemes (Figs. S5–S12, Table S5, Fig. S3, Fig. S13 online). Collectively, our results provide insights into the nontrivial interdependencies of SC and FC, highlighting their cognitive significance and the molecular mechanisms underlying the connectome of connectomes (For a detailed discussion, see Supplementary Materials). Future studies could further investigate whether and how the interactive SC-FC connectome changes with disease, in particular identifying the nodes responsible for communication between these two networks and whether these nodes undergo role changes in patients with brain disorders. It would also be interesting to investigate the age-related changes in the interdependent relationship between the SC and FC.

Conflict of interest

The authors declare that they have no conflict of interest.

Acknowledgments

This study was supported by the National Natural Science Foundation of China (82021004, 82327807 and T24B2012), Beijing Natural Science Foundation (JQ23033) and the Fundamental Research Funds for the Central Universities (2233100018 and 2233300002). We thank Dr. Tianyuan Lei for the discussion on the experimental design. The imaging data were provided by the Human Connectome Project, WU-Minn Consortium (Principal Investigators: David Van Essen and Kamil Ugurbil; 1U54MH091657) funded by the 16 NIH Institutes and Centers which support the NIH Blueprint for Neuroscience Research; and by the Mc-Donnell Center for Systems Neuroscience at Washington University.

Author contributions

Xiaoyue Wang and Lianglong Sun performed the analyses. Yong He, Xiaoyue Wang, and Lianglong Sun designed the study and wrote the manuscript. Yong He and Lianglong Sun supervised the study and developed the main concepts. Yong He, Xiaoyue Wang, and Lianglong Sun interpreted results and contributed to the reviewing and editing of the manuscript. Xinyuan Liang, Mingrui Xia, Tengda Zhao, and Xuhong Liao provided assistance in experimental design, data processing and analysis, and interpretation of results. Yong He provided the secured funding.

Data availability

The HCP dataset is available in the HCP ConnectomeDB (https://db.humanconnectome.org/), the neurocognitive flexibility dataset (https://surfer.nmr.mgh.harvard.edu/fswiki/BrainmapOntology_Yeo2015), neurotransmitter dataset (https://github.com/netneurolab/hansen_receptors), and AHBA dataset (https://human.brain-map.org/static/download) are all publicly available. Intermediate data and analysis code are available at https://github.com/wang-xyue/Topographic-cognitive-neurobiological-profiling-of-interdependent-SC-FC.

Appendix A. Supplementary material

Supplementary data to this article can be found online at https://doi.org/10.1016/j.scib.2025.02.029.

References

[1] Suárez LE, Markello RD, Betzel RF, et al. Linking structure and function in macroscale brain networks. Trends Cogn Sci 2020;24:302–15.

[2] Wang Z, Dai Z, Gong G, et al. Understanding structural-functional relationships in the human brain: a large-scale network perspective. Neuroscientist 2015;21:290–305.
[3] Fotiadis P, Parkes L, Davis KA, et al. Structure–function coupling in macroscale human brain networks. Nat Rev Neurosci 2024;25:688–704.
[4] Buldyrev SV, Parshani R, Paul G, et al. Catastrophic cascade of failures in interdependent networks. Nature 2010;464:1025–8.
[5] Battiston F, Nicosia V, Chavez M, et al. Multilayer motif analysis of brain networks. Chaos 2017;27:047404.
[6] Breedt LC, Santos FAN, Hillebrand A, et al. Multimodal multilayer network centrality relates to executive functioning. Netw Neurosci 2023;7:299–321.
[7] Battiston F, Guillon J, Chavez M, et al. Multiplex core-periphery organization of the human connectome. J R Soc Interface 2018;15:20180514.
[8] Lim S, Radicchi F, van den Heuvel MP, et al. Discordant attributes of structural and functional brain connectivity in a two-layer multiplex network. Sci Rep 2019;9:2885.
[9] Van Essen DC, Smith SM, Barch DM, et al. The wu-minn human connectome project: an overview. Neuroimage 2013;80:62–79.
[10] Glasser MF, Coalson TS, Robinson EC, et al. A multi-modal parcellation of human cerebral cortex. Nature 2016;536:171–8.
[11] Mucha PJ, Richardson T, Macon K, et al. Community structure in time-dependent, multiscale, and multiplex networks. Science 2010;328:876–8.
[12] Liao X, Cao M, Xia M, et al. Individual differences and time-varying features of modular brain architecture. Neuroimage 2017;152:94–107.
[13] Yeo BT, Krienen FM, Eickhoff SB, et al. Functional specialization and flexibility in human association cortex. Cereb Cortex 2015;25:3654–72.
[14] Hansen JY, Shafiei G, Markello RD, et al. Mapping neurotransmitter systems to the structural and functional organization of the human neocortex. Nat Neurosci 2022;25:1569–81.
[15] Hawrylycz MJ, Lein ES, Guillozet-Bongaarts AL, et al. An anatomically comprehensive atlas of the adult human brain transcriptome. Nature 2012;489:391–9.